Intracellular Delivery

DOI: 10.1002/anie.201206595

A Bioreducible Polymer for Efficient Delivery of Fas-Silencing siRNA into Stem Cell Spheroids and Enhanced Therapeutic Angiogenesis**

*Min Suk Shim, Suk Ho Bhang, Kyunghwan Yoon, Kyunghee Choi, and Younan Xia**

Adult mesenchymal stem cells (MSCs) hold great potential for the treatment of ischemic disease because they can contribute to angiogenesis by secreting a broad spectrum of angiogenic growth factors.[1] However, the low survival rate and poor engraftment of the transplanted MSCs limit the use of MSC-based therapy in a clinical setting.[2] Recently, it was shown that transplanting stem cells as spheroids of approximately 200 μm in diameter could be a promising strategy for improving their angiogenic efficacy.[3] The mild hypoxic condition established in the core of a spheroid (arising from the limited diffusion of nutrients and oxygen) can precondition the cells to an ischemic environment.[4] Through this natural preconditioning, the cells can acquire resistance to the hypoxic condition by increasing the production of various growth factors that are necessary for survival.[4,5] However, for MSC-based spheroids, the therapeutic efficacy of this approach is limited by the number of MSCs that could be included in the spheroids. When the size of the spheroid was increased beyond a certain value, a large number of MSCs in the core underwent severe hypoxia and eventually died (results not shown here). As a result, there is a strong need to develop an effective method for increasing the survival rate of MSCs in a large spheroid to enhance their therapeutic efficacy.

One way to improve the survival rate of MSCs in a spheroid is to inhibit their apoptosis, which is activated by interactions between Fas and its ligand (FasL).[6] It was reported that inhibition of Fas expression could protect the cells from apoptosis.[7] Based on this notion, we hypothesized that hypoxia-induced apoptosis in a spheroid could be mitigated by inhibiting Fas expression through the delivery of Fas-silencing small interfering RNA (Fas siRNA), resulting in successful formulation of spheroids with enlarged sizes. Because of the increased number of viable MSCs and thereby augmented total secretion of paracrine angiogenic factors, the enlarged spheroids were anticipated to significantly enhance angiogenesis. In recent years, various cationic polymers have been actively explored as efficient nonviral vectors because they can strongly condense negatively charged siRNAs and protect them from degradation by nucleases.[8] However, the use of a high-molecular-weight cationic polymer such as polyethylenimine (PEI, a commercially available transfecting agent) is problematic because of its non-biodegradability and thus high cytotoxicity.[9] As a result, stimuli-responsive, biodegradable polymers have recently emerged as effective nonviral carriers for reducing cytotoxicity and thus enhancing transfection efficiency by taking advantage of cellular stimuli-responsive degradation and efficient release of nucleic acids.[10]

In this study, branched poly(disulfide amine) (B-PDA), a bioreducible cationic polymer containing disulfide bonds in the backbone, was developed for efficient intracellular delivery of Fas siRNA into human MSCs (hMSCs). The salient features of this polymer include: 1) efficient complexation of flexible cationic amino branches with Fas siRNA; 2) high proton-buffering capacity for efficient endosomal escape because the cationic branches are consisted of primary, secondary, and tertiary amines with a broad range of pK_a values, which represents a major advantage compared to the previously reported bioreducible polymers;[10c,d] 3) facilitated release of Fas siRNA in the cytoplasm, an intracellular target site for RNA interference (RNAi), because of rapid degradation of disulfide bonds in the reductive environment; and 4) low toxicity and efficient body clearance owing to efficient biodegradation. As shown in Figure 1a, bioreducible B-PDA can be used to complex with Fas siRNA and release it in the cytoplasm of an hMSC. The Fas-silenced hMSCs can then be formulated as enlarged spheroids and transplanted into mouse ischemic hind limbs as paracrine secretors for therapeutic angiogenesis.

The synthesis of B-PDA involved polymerization of a Boc-protected oligoamine monomer (Boc = *tert*-butoxycarbonyl) and disulfide-bearing *N*,*N*′-cystaminebisacrylamide by Michael addition, followed by deprotection of the Boc groups (see Figure S1 in the Supporting Information for details). As determined by gel-permeation chromatography (GPC), the B-PDA had molecular weights of $M_n \approx 6.0$ kDa and

[*] Dr. M. S. Shim,[+] Dr. S. H. Bhang,[+] Dr. K. Yoon, Prof. Y. Xia
Department of Biomedical Engineering, Washington University
St. Louis, MO 63130 (USA)
E-mail: younan.xia@bme.gatech.edu
Prof. K. Choi
Department of Pathology and Immunology
Washington University School of Medicine
St. Louis, MO 63110 (USA)
Dr. M. S. Shim,[+] Dr. S. H. Bhang,[+] Prof. Y. Xia
Current address: The Wallace H. Coulter Department of Biomedical Engineering, Georgia Institute of Technology and Emory University; School of Chemistry & Biochemistry and School of Chemical & Biomolecular Engineering, Georgia Institute of Technology
Atlanta, GA 30332 (USA)
[+] These authors contributed equally to this work.

[**] This work was supported in part by an NIH Director's Pioneer Award (DP1 OD000798 to Y.X.) and NIH grants from the National Heart, Lung and Blood Institute (NHLBI, R01 HL55337 and R01 HL63736 to K.C.). We thank Dennis Oakley of the Bakewell Neuroimaging Core at Washington University School of Medicine for assistance with the confocal microscopy imaging.

Supporting information for this article is available on the WWW under http://dx.doi.org/10.1002/anie.201206595.

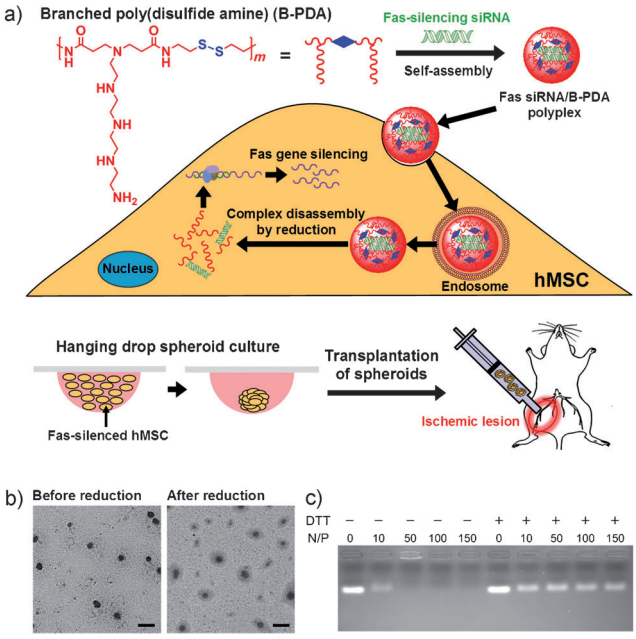

Figure 1. a) Intracellular trafficking of Fas siRNA/B-PDA polyplexes for the delivery of Fas siRNA into hMSCs and formation of enlarged spheroids of Fas-silenced hMSCs for ischemia treatment. b) TEM images of siRNA/B-PDA polyplexes before and after reduction at 37 °C for 8 h in the presence of DTT (10 mM). The scale bars correspond to 200 nm. c) Gel retardation assay of siRNA/B-PDA polyplexes obtained under varying N/P ratios before and after incubation with DTT (10 mM) at 37 °C for 4 h.

$M_w \approx 7.4$ kDa, together with a narrow polydispersity index of 1.23. The B-PDA exhibited a high proton-buffering capacity comparable to branched PEI, as demonstrated by the titration curves (Figure S2). This result implies that the Fas siRNA/B-PDA polyplexes should be able to escape from the acidic endosome by the hypothetical "proton-buffering effect" after they have entered cells.[11]

The redox-sensitive degradation of B-PDA was investigated by monitoring its molecular weights after incubation in a 10 mM aqueous solution of dithiothreitol (DTT) for different periods of time. Our results indicate that the B-PDA could be completely degraded into short segments with M_w less than 600 Da within 3 h under the reductive conditions (Figure S3a in the Supporting Information). The multiple amino groups on the flexible branches of B-PDA could efficiently complex with negatively charged Fas siRNA to form stable polyplexes with varying amine to phosphate (N/P) ratios. As shown by TEM images (Figure 1b, left), compact Fas siRNA/B-PDA polyplexes with diameters in the range of 60–80 nm were formed at an N/P ratio of 100. After incubation in reductive DTT solution, the Fas siRNA/B-PDA polyplexes became dramatically loosened (Figure 1b, right). The destabilization of Fas siRNA/B-PDA polyplexes after reduction was also confirmed by dynamic light scattering analysis (Figure S3b). A gel electrophoresis assay also demonstrated the redox-triggered disassembly of the Fas siRNA/B-PDA polyplexes (Figure 1c). It is well-known that intracellular localization and disassembly of Fas siRNA from a carrier determine the efficiency of RNAi.[12] For the Fas siRNA/B-PDA polyplexes, we confirmed their efficient disassembly inside hMSCs by confocal laser scanning microscopy. As represented by many red dots in the confocal micrograph (Figure S3c), a significant amount of free siRNA (labeled with the Cy3 dye) was released from the polymer chains labeled with Alexa Fluor 488 (green dots). This result confirms that the redox-sensitive degradation of disulfide bonds in B-PDA facilitated the cytoplasmic release of Fas siRNA.

The Fas silencing efficiencies of various types of Fas siRNA/polymer polyplexes or naked siRNA were determined by incubating them with hMSCs for 48 h. For Fas siRNA/B-PDA polyplexes, an N/P ratio of 100 was used, which was optimized by considering their Fas silencing efficiency and cytotoxicity. Branched PEI (25 kDa, N/P ratio of 10) was used as a nonreducible control. The transfected hMSCs were cultured as spheroids under hypoxic conditions (e.g., 1% oxygen and serum-free medium) by using a hanging drop method (see the Supporting Information for details) to mimic the in vivo ischemic environment. As shown in Figure 2a, b, the level of Fas messenger RNA (Fas mRNA) was substantially suppressed by the Fas siRNA/B-PDA polyplexes. Importantly, the gene silencing efficiency of Fas siRNA/B-PDA polyplexes was about 1.5 times higher than that of Fas siRNA/PEI polyplexes (Figure 2b). It is known that highly stable complexation of siRNA with nondegradable PEI limits the dissociation of siRNA from the PEI polyplexes.[13] Therefore, the more efficient inhibition of Fas expression by the B-PDA relative to PEI can be attributed to its capability to facilitate the cytoplasmic release of Fas siRNA (Figure S3c in the Supporting Information).

The effect of Fas inhibition by Fas siRNA/B-PDA polyplexes on the apoptosis of hMSCs was investigated by quantifying mRNA expressions of anti-apoptotic Bcl-XL and pro-apoptotic Bax (Figure 2a, c, d). Efficient inhibition of Fas expression by siRNA/B-PDA polyplexes led to concomitantly increased Bcl-XL expression and decreased Bax expression, thus demonstrating significantly down-regulated Fas-inductive apoptosis gene cascades. In addition, Fas siRNA/B-PDA polyplexes significantly down-regulated caspase-3, a protease involved in Fas-mediated apoptosis (Figure S4a, b in the Supporting Information).[14] As a result, treatment with Fas siRNA/B-PDA polyplexes greatly increased the viability of hMSCs in the spheroids as compared to other groups (Figure 2e and Figure S4c, d). The substantially inhibited apoptosis of hMSCs by Fas siRNA/B-PDA polyplexes also affected the morphologies of their spheroids. As shown by SEM images (Figure 2f and Figure S5), hMSCs treated with Fas siRNA/B-PDA polyplexes were successfully formulated as enlarged spheroids because of their reinforced anti-apoptotic activity, even under severe hypoxic conditions in the spheroid core. A majority of the enlarged spheroids had diameters in the range of 800–1000 μm. Although hMSCs treated with Fas siRNA/PEI polyplexes could also be cultured as enlarged spheroids with similar diameters, most of them showed apoptotic core deformation. The spheroids formed with hMSCs without any treatment or treated with naked Fas siRNA easily dissociated into individual cells because of severe hypoxic conditions caused by both inner and outer microenvironments.

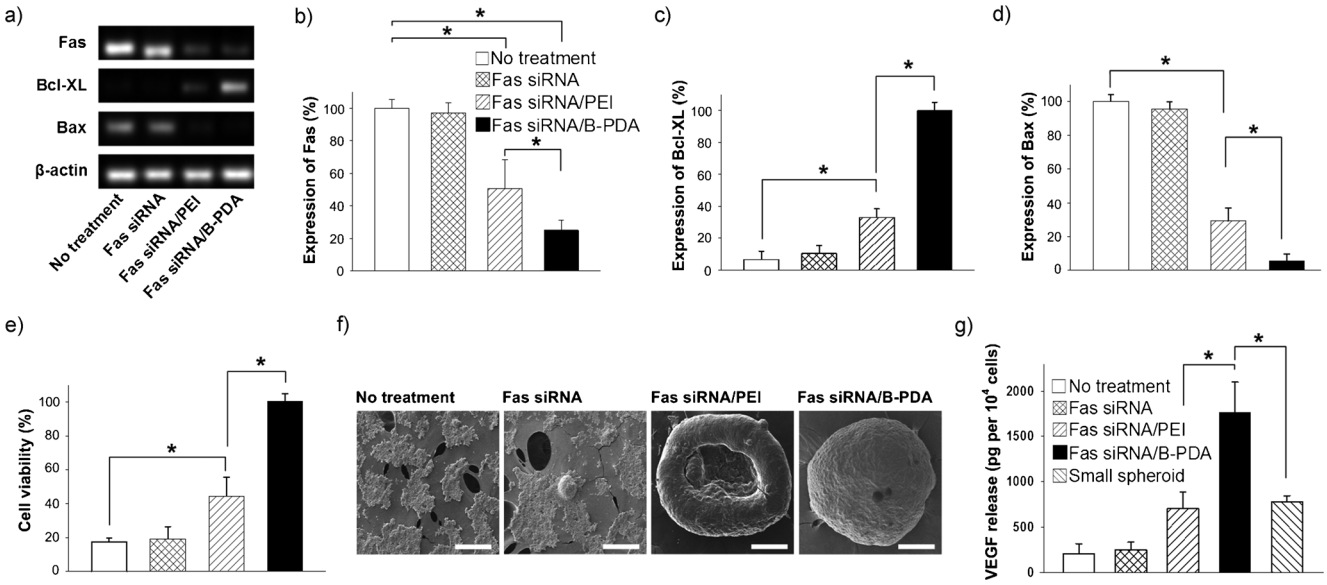

Figure 2. Anti-apoptotic activity of the enlarged hMSC spheroids treated with Fas siRNA by different delivery methods, as determined by a) reverse transcription-polymerase chain reaction (RT-PCR) and b–d) quantitative PCR (qPCR). e) Cell viability of hMSC spheroids treated with Fas siRNA by different delivery methods, as determined by neutral red assay. The results are expressed as percentages relative to the Fas siRNA/B-PDA group. f) SEM images of hMSC spheroids treated with Fas siRNA via different delivery methods under hypoxic culture. Scale bars correspond to 200 μm. g) Quantification of VEGF secreted from hMSC spheroids after treatment with various Fas siRNA delivery methods, as quantified by enzyme-linked immunosorbent assay (ELISA). The hMSC spheroids were cultured under hypoxic conditions for 5 days. * denotes $p < 0.05$.

The enlarged hMSC spheroids treated with Fas siRNA/B-PDA polyplexes significantly increased the expression of hypoxia-induced survival factor (i.e., HIF-1α) and anti-apoptotic, angiogenic growth factors, including vascular endothelial growth factor (VEGF), fibroblast growth factor 2 (FGF2), and hepatocyte growth factor (HGF; Figure S6a–f in the Supporting Information). HIF-1α has been known to stimulate the production of angiogenic growth factors, as well as to trigger anti-apoptotic signaling cascades.[15] Therefore, the increased secretion of VEGF, FGF2, and HGF in the hMSC spheroids treated with Fas siRNA/B-PDA polyplexes seems to be related to the increased expression of HIF-1α. It is worth noting that the amount of secreted angiogenic factors per individual hMSC for enlarged hMSC spheroids treated with Fas siRNA/B-PDA polyplexes was much higher (about two times higher) than that of small hMSC spheroids (diameters ranging from 250 to 350 μm) that were not treated with Fas siRNA (Figure 2g and Figure S6g,h). The enhanced paracrine secretion of enlarged hMSC spheroids can be attributed to the substantial increase in HIF-1α expression because of their exposure to greater hypoxic conditions compared to the small counterparts.

To determine if the enhanced viability of hMSCs in the enlarged spheroids with Fas siRNA transfection (enlarged spheroids (+siRNA)) and their increased secretion of paracrine angiogenic factors can stimulate therapeutic angiogenesis, we evaluated their in vivo angiogenic efficacy in a mouse model of hind-limb ischemia. For comparison, we also prepared and transplanted the following samples: enlarged hMSC spheroids formulated with the same initial number of hMSCs without Fas siRNA transfection (enlarged spheroids (−siRNA)), Fas siRNA-transfected hMSC spheroids with a small number of hMSCs (small spheroids (+siRNA)), and small hMSC spheroids without Fas siRNA transfection (small spheroids (−siRNA)). The reason for including small spheroid (+siRNA) and small spheroids (−siRNA) was to evaluate the effects of the number of hMSCs and the Fas siRNA-mediated anti-apoptosis on the angiogenic efficacy of the spheroids, respectively. It should be noted that the enlarged spheroids (−siRNA) could not remain as spheroids because of severe hypoxia-induced apoptosis. Prior to the in vivo study, the bioactivity of growth factors secreted from the enlarged spheroids (+siRNA) was confirmed by the significantly reduced apoptosis of human umbilical vein endothelial cells (HUVECs) cultured in the conditioned medium obtained from the enlarged spheroids (+siRNA; see Figure S7 for details). The sustained retention of transplanted hMSCs as paracrine secretors is critical to their effectiveness in angiogenesis. Anti-apoptosis and cell survival of transplanted hMSC spheroids in mouse ischemic tissues were evaluated by double immunofluorescent staining of caspase-3 and anti-human nuclear antigen (HNA) in the tissues. When enlarged spheroids (+siRNA) were transplanted, a significantly larger number of hMSCs survived in the ischemic tissues compared to other types of spheroids (Figure S8). Interestingly, there was no statistical difference in anti-apoptosis and cell survival of hMSCs between small spheroids (+siRNA) and small spheroids (−siRNA) groups (Figure S8b,c). This finding implies that Fas siRNA treatment is not effective for small hMSC spheroids because the survival of a small number of hMSCs can be effectively maintained by forming spheroids.

We also evaluated the therapeutic angiogenic efficacies of various types of hMSC spheroids in mouse ischemic hind

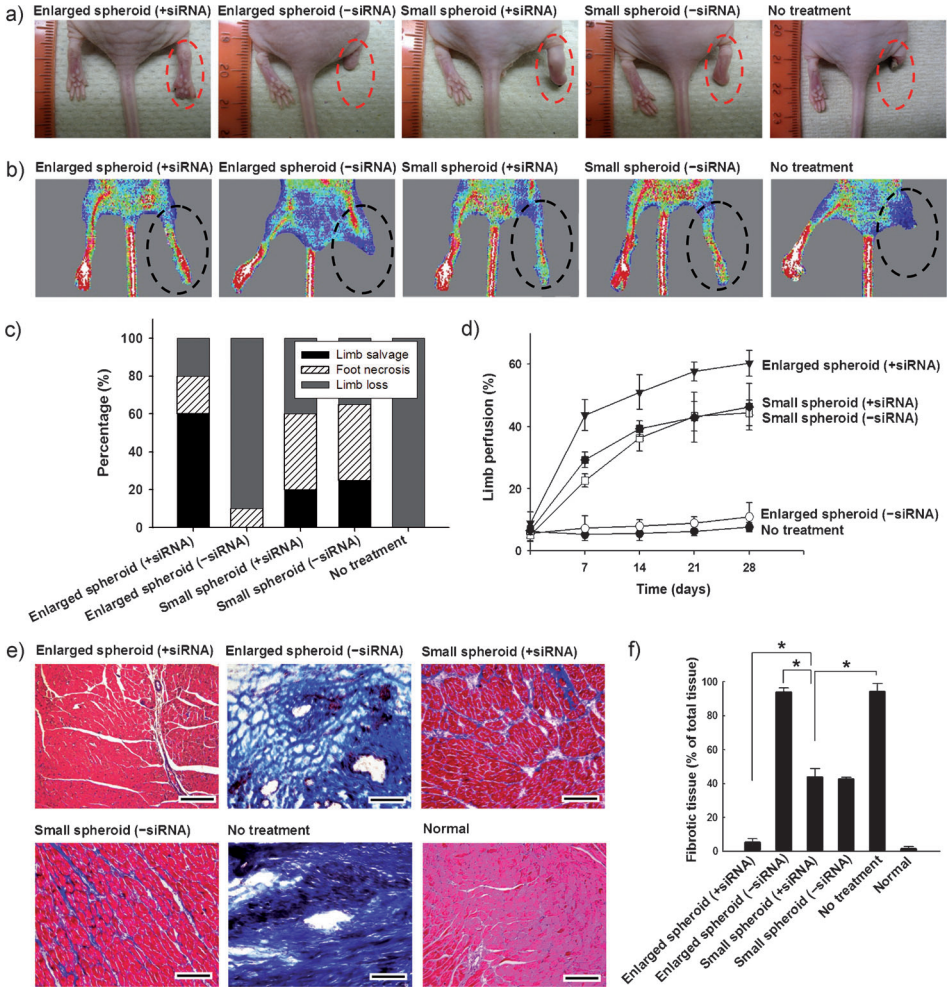

Figure 3. Improvements of ischemic hind-limb salvage 28 days post transplantation of various types of hMSC spheroids. a) Representative photographs and b) laser Doppler perfusion images of the ischemic hind limbs 28 days post treatment. Dashed eclipses indicate ischemic hind limbs. c) Physiological status of ischemic limbs 28 days post treatment. d) Blood perfusion ratio of ischemic limbs measured by laser Doppler imaging 0, 7, 14, 21, and 28 days post treatment. The ratio of blood perfusion between ischemic and normal limbs was significantly improved by the enlarged spheroids (+siRNA) at all time points. e) Masson's trichrome staining (×100) of ischemic tissues (red: normal muscle tissues; blue: fibrotic tissues) and f) evaluation of fibrotic tissue area in the ischemic tissues 28 days post treatment. It should be noted that the enlarged spheroids (−siRNA) could not remain as spheroids because of intolerable hypoxia-induced apoptosis. The scale bars correspond to 50 μm. All photographs have the same magnification. * denotes $p < 0.05$.

limbs by their physiological status, laser Doppler perfusion imaging, and histological analysis (Figure 3). As shown in Figure 3a,c, the limb muscles of mice treated with enlarged spheroids (+siRNA) were effectively protected against ischemic damage, whereas all of the untreated mice with ischemic hind limbs showed rapid limb necrosis and complete limb loss by autoamputation by day 28. The mice treated with enlarged spheroids (+siRNA) underwent a significantly reduced limb loss rate (ca. 20%) compared with other groups. Laser Doppler perfusion imaging revealed that the blood perfusion in the ischemic limbs treated with enlarged spheroids (+siRNA) was significantly improved compared to other groups (Figure 3b,d). Histological analysis also revealed that the ischemic limbs treated with enlarged spheroids (+siRNA) showed substantially reduced tissue degeneration and fibrosis when compared with other groups (Figure 3e,f, and Figure S9).

The transplantation of enlarged spheroids (+siRNA) significantly improved the formation of both arterioles and capillaries when compared to other types of hMSC spheroids (Figure 4). The transplantation of enlarged spheroids (+siRNA) also induced the formation of new microvessels most efficiently compared to other groups, as evident from a significantly increased number of BrdU-positive cells (Figure 4d). In addition, expressions of intercellular adhesion molecule (ICAM) and vascular cell adhesion molecule (VCAM) were the highest for the ischemic tissues treated with enlarged spheroids (+siRNA) (Figure S10a). Enhanced secretion of paracrine factors from the enlarged spheroids (+siRNA) might have activated the host cells to express more adhesion molecules. The increase in ICAM and VCAM expressions for the activated host cells might promote the recruitment of endothelial progenitor cells to ischemic sites and contribute to neovascularization.

To validate our hypothesis that the enhanced angiogenic efficiency of enlarged hMSC spheroids is closely correlated with their increased secretion of angiogenic and anti-apoptotic growth factors, expressions of human VEGF (hVEGF) and human FGF2 (hFGF2) secreted from various hMSC spheroids were assessed 28 days after transplantation (Figure S10b). The highest levels of hVEGF and hFGF2 expressions were observed in mice that received enlarged spheroids (+siRNA), whereas hVEGF and hFGF2 expressions were not detected in mice transplanted with enlarged spheroids (−siRNA; (Figure S10b). We also quantified the expressions of human specific SM-α actin and CD31 to evaluate if microvessels were directly derived from hMSCs. Importantly, we did not observe noticeable expressions of human specific SM-α actin and CD31, thus confirming that the enhanced angiogenesis was mainly caused by the increased secretion of paracrine angiogenic factors from the enlarged hMSC spheroids (Figure S10b).

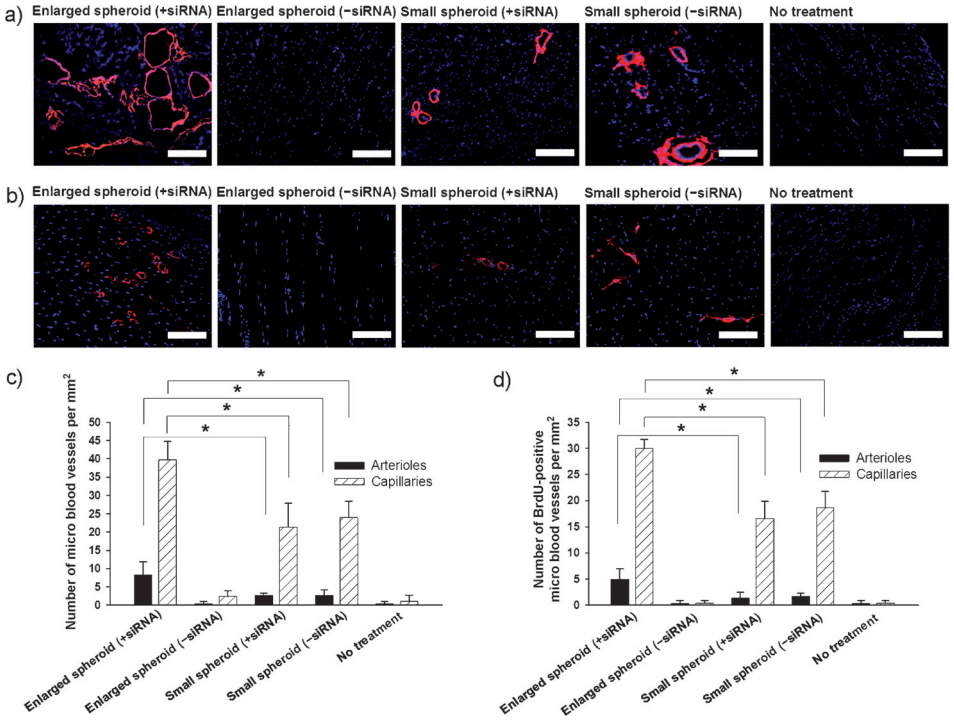

Figure 4. Immunofluorescent staining of a) SM-α actin (staining of arterioles) and b) CD31 (staining of capillaries) in the ischemic limb tissues 28 days post transplantation. Nuclei of the cells were counter-stained in blue with DAPI. The scale bars correspond to 100 μm. Quantification of c) total arteriole and capillary density and d) BrdU-positive arteriole and capillary density in the ischemic regions. * denotes $p < 0.05$.

In summary, we have shown that Fas siRNA delivery into hMSCs by bioreducible B-PDA successfully suppressed Fas expression and thus led to effective inhibition of hypoxia-induced apoptosis in the enlarged hMSC spheroids (Figure S11). The enlarged hMSC spheroids significantly enhanced angiogenesis in mouse ischemic hind limbs. This study demonstrates that an interdisciplinary approach of integrating sequence-specific RNAi, nonviral gene delivery, and spheroid-based stem cell delivery may offer a powerful therapeutic tool for the efficient treatment of ischemic disease.

Received: August 15, 2012
Published online: October 16, 2012

Keywords: intracellular delivery · polymers · nanoparticles · stem cells · RNA interference

[1] a) P. Bianco, M. Riminucci, S. Gronthos, P. G. Robey, *Stem Cells* **2001**, *19*, 180–192; b) A. I. Caplan, J. E. Dennis, *J. Cell. Biochem.* **2006**, *98*, 1076–1084; c) T. Kinnaird, E. Stabile, M. S. Burnett, C. W. Lee, S. Barr, S. Fuchs, S. E. Epstein, *Circ. Res.* **2004**, *94*, 678–685.

[2] E. Tateishi-Yuyama, H. Matsubara, T. Murohara, U. Ikeda, S. Shintani, H. Masaki, K. Amano, Y. Kishimoto, K. Yoshimoto, H. Akashi, K. Shimada, T. Iwasaka, *Lancet* **2002**, *360*, 427–435.

[3] S. H. Bhang, S.-W. Cho, W.-G. La, T.-J. Lee, H. S. Yang, A.-Y. Sun, S.-H. Baek, J.-W. Rhie, B.-S. Kim, *Biomaterials* **2011**, *32*, 2734–2747.

[4] T. Korff, S. Kimmina, G. Martiny-Baron, H. G. Augustin, *FASEB J.* **2001**, *15*, 447–457.

[5] L. Gaedtke, L. Thoenes, C. Culmsee, B. Mayer, E. Wagner, *J. Proteome Res.* **2007**, *6*, 4111–4118.

[6] a) E. Song, S.-K. Lee, J. Wang, N. Ince, N. Ouyang, J. Min, J. Chen, P. Shankar, J. Lieberman, *Nat. Med.* **2003**, *9*, 347–351; b) W. Suarez-Pinzon, O. Sorensen, R. C. Bleackley, J. F. Elliott, R. V. Rajotte, A. Rabinovitch, *Diabetes* **1999**, *48*, 21–28; c) D. Kagi, F. Vignaux, B. Ledermann, K. Burki, V. Depraetere, S. Nagata, H. Hengartner, P. Golstein, *Science* **1994**, *265*, 528–530.

[7] P. Hamar, E. Song, G. Kökény, A. Chen, N. Ouyang, J. Lieberman, *Proc. Natl. Acad. Sci. USA* **2004**, *101*, 14883–14888.

[8] a) N. P. Gabrielson, H. Lu, L. Yin, D. Li, F. Wang, J. Cheng, *Angew. Chem.* **2012**, *124*, 1169–1173; *Angew. Chem. Int. Ed.* **2012**, *51*, 1143–1147; b) T. G. Park, J. H. Jeong, S. W. Kim, *Adv. Drug Delivery Rev.* **2006**, *58*, 467–486.

[9] a) D. Fischer, T. Bieber, Y. Li, H. Elsässer, T. Kissel, *Pharm. Res.* **1999**, *16*, 1273–1279; b) M. J. Knauf, D. P. Bell, P. Hirtzer, Z.-P. Luo, J. D. Young, N. V. Katre, *J. Biol. Chem.* **1988**, *263*, 15064–15070.

[10] a) D. M. Lynn, R. Langer, *J. Am. Chem. Soc.* **2000**, *122*, 10761–10768; b) Y.-L. Lin, G. Jiang, L. K. Birrell, M. E. H. El-Sayed, *Biomaterials* **2010**, *31*, 7150–7166; c) L. V. Christensen, C.-W. Chang, W. J. Kim, S. W. Kim, *Bioconjugate Chem.* **2006**, *17*, 1233–1240; d) R. S. Burke, S. H. Pun, *Bioconjugate Chem.* **2010**, *21*, 140–150.

[11] O. Boussif, F. Lezoualc'h, M. A. Zanta, M. D. Mergny, D. Scherman, B. Demeneix, J. P. Behr, *Proc. Natl. Acad. Sci. USA* **1995**, *92*, 7297–7301.

[12] A. Detzer, M. Overhoff, W. Wünsche, M. Rompf, J. J. Turner, G. D. Ivanova, M. J. Gait, G. Sczakiel, *RNA* **2009**, *15*, 627–636.

[13] M. Breunig, C. Hozsa, U. Lungwitz, K. Watanabe, I. Umeda, H. Kato, A. Goepferich, *J. Controlled Release* **2008**, *130*, 57–63.

[14] D. W. Nicholson, A. Ali, N. A. Thornberry, J. P. Vaillancourt, C. K. Ding, M. Gallant, Y. Gareau, P. R. Griffin, M. Labelle, Y. A. Lazebnik, N. A. Munday, S. M. Raju, M. E. Smulson, T.-T. Yamin, V. L. Yu, D. K. Miller, *Nature* **1995**, *376*, 37–43.

[15] a) M. Bernaudin, A. S. Nedelec, D. Divoux, E. T. MacKenzie, E. Petit, P. Schumann-Bard, *J. Cereb. Blood Flow Metab.* **2002**, *4*, 393–403; b) D. Ma, T. Lim, J. Xu, H. Tang, Y. Wan, H. Zhao, M. Hossain, P. H. Maxwell, M. Maze, *J. Am. Soc. Nephrol.* **2009**, *20*, 713–720.

